Phosphorescence Mechanisms. I. Approach and General Analysis

C. BILLINGTON
Division of Chemical Physics, Commonwealth Scientific and Industrial Research Organization, Chemical Research Laboratories, Melbourne, Australia

(Received June 13, 1960)

A new technique is described for the study of decay mechanisms in phosphors. When a phosphor is excited by radiation whose intensity is modulated to a depth less than 10%, the modulation of the emission intensity has negligible harmonic content. Quantitative comparisons of these two modulated signals, if of sufficient accuracy and range, result in qualitative distinctions between different basic mechanisms, and the possibility of subsequent quantitative analysis. In particular monomolecular and bimolecular processes are unequivocally distinguished.

INTRODUCTION

THE present contribution, which is the result of both experimental and theoretical development over several years, provides a new approach to the problem of the measurement and analysis of phosphorescence decay. It originated in the work of Lord and Rees,[1] who used sinusoidally modulated excitation. They were concerned to distinguish between simple monomolecular and simple bimolecular mechanisms on the basis of the relationship between the phase shift of the emitted modulation and its ratio of maximum to minimum intensity. Their experimental arrangement permitted only a single frequency of modulation.

It will be argued here that by variation of the modulation frequency and accurate comparison between the modulation parameters of the exciting and emitted radiations, it is possible to resolve a number of simple "monomolecular" processes acting together in the same phosphor, independently of whether the actual mechanisms of phosphorescence are in fact monomolecular or bimolecular. This last question can be explored by varying the average exciting intensity in addition. The work is conveniently divided into four parts. Part I is a general statement and analysis of the approach and its possibilities. Some of the conceptions are outside the accustomed field of solid-state physics, and the introduction of a few new terms has been inevitable. Part II is devoted to a description of the equipment. As the success of the whole thesis is heavily dependent upon the accuracy and reliability of the observations, it is essential to justify the experimental method. In Part III the method of numerical analysis is treated, and the resolving power of the equipment is assessed quantitatively. Part IV gives the results of analyses applied to three phosphors, and discusses some of the implications.

THE MONOMOLECULAR CASE

Many authors have produced equivalent mathematical analyses of the monomolecular case, and it is reproduced here only for the sake of completeness and definition.

A monomolecular process is said to operate when transitions accompanied by emission are spontaneous, and are defined sufficiently by their probability per second α, which is called the decay rate constant for the bulk material. The differential equation describing the process in a small volume of crystal is

$$dN/dt=\tilde{I}(t)-\alpha N, \tag{1}$$

where N is the number of electrons in the state from which emission takes place at time t, and $\tilde{I}(t)$ is the number of electrons being excited to that state per second by external means. The quantities $\tilde{I}(t)$ and αN are evidently closely related to the observable intensities of excitation and emission.

If $\tilde{I}$ has the form of a single step, Eq. (1) is immediately soluble, and N approaches its second equilibrium value exponentially. Equation (1) is also exactly soluble for sinusoidally modulated excitation which may be written

$$\tilde{I}(t)=\tilde{A}\{1+a\cos\omega t\}, \tag{2}$$

where a is the depth of modulation, ω is the modulation pulsatance, and $\tilde{A}$ is the average value of $\tilde{I}$. The steady-state solution shows that the number of electrons returning to the ground state per second is

$$\alpha N=\tilde{A}\{1+a\lambda\cos(\omega t+\phi)\}. \tag{3}$$

The attenuation factor λ, and the phase retardation ϕ, are given by the relations

$$\lambda=\alpha/(\alpha^2+\omega^2)^{\frac{1}{2}}, \tag{4}$$

and

$$\phi=\tan^{-1}(\omega/\alpha). \tag{5}$$

Circular functions of the argument ωt in the modulation part of the excitation function (also linear combinations of them) are undistorted by a monomolecular process whose transmission function is independent of both $\tilde{A}$ and a. Furthermore, the parameters λ and ϕ are not mutually independent. A simple monomolecular process is confirmed if either parameter can be treated as the observable, and the appropriate relation (4) or (5) verified over a wide frequency range. A combination of both parameters, which we may call the *in-phase* attenuation factor χ, leads to a simpler analysis. From

[1] M. P. Lord and A. L. G. Rees, Proc. Phys. Soc. (London) 58, 280 (1946).

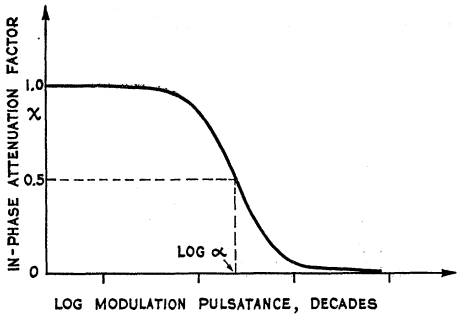

FIG. 1. The form of relation (6), $\chi=\alpha^2/(\alpha^2+\omega^2)$ which arises from a simple monomolecular process.

relations (4) and (5) we have

$$\chi=\lambda\cos\phi=\alpha^2/(\alpha^2+\omega^2). \tag{6}$$

It will be observed that only the ratio ω/α appears in the relations (4), (5), and (6). Accordingly, the shape of the representation on a logarithmic scale of pulsatance is independent of the value of the rate constant. Relation (6) which is illustrated graphically in Fig. 1 has the additional advantage of a center of symmetry at the point $[\frac{1}{2}, \log\alpha]$.

EXPERIMENTAL ASPECT

In practice it is convenient to use a powdered phosphor, and to sample the excitation and emission intensities using photoelectric detectors which give electrical signals defined by

$$I_{\text{exc}}=A\{1+a\cos\omega t\},$$

and

$$I_{\text{em}}=B\{1+\alpha\lambda\cos(\omega t+\phi)\}.$$

The same symbols a, λ, ϕ, and χ may be used provided there is proportionality between instantaneous values of both I_{exc} and $\tilde{I}$, and I_{em} and αN. The requirement of *instantaneous* proportionality formally excludes processes of finite rate in cascade with the process "α", but if they are very fast in comparison the condition is still closely fulfilled for experimental purposes.

Frequency is normally conceived on a logarithmic scale, even though its measurement may consist of a counting operation. Frequency stability and measuring accuracy of the order 0.01% are readily achieved over many orders of magnitude. On the scale of Fig. 1 this corresponds to a uniform uncertainty of less than 1 μ in the horizontal direction for a measured point. The range of frequency is limited by the feasibility of modulating the source of excitation. With the present experimental arrangement the depth of modulation is limited to 10% ($a=0.1$), and nearly four decades are accessible from 3 cycles/sec upwards with harmonic distortion of less than 1%.

The in-phase attenuation factor χ is measured by a homodyne technique using a bandwidth of about 0.1 cycle/sec. Under convenient operating conditions the noise level is about 0.001 for all values of χ. Consequently when χ is plotted linearly as in Fig. 1, the vertical uncertainty is also constant, and is equal to about 0.001 in. in the figure.

Thus the representation of observables in Fig. 1 hereafter called a *phosphorogram* is experimentally practicable and analytically simple. It has the advantage over the ($\log I$, t) representation, commonly used for measurements on a Becquerel's phosphoroscope, that the error can be made small and constant throughout a useful range of the observables (χ, $\log\omega$).

The complete *phosphorometer* is described in Part II.

THE BIMOLECULAR CASE

When absorption of the excitation energy leads to ionization of the luminescent center, luminescence may result from a recombination of an electron with a center. In the simplest case which is that of an insulator, the emission probability is proportional to the square of the number of mobile electrons. The process is described by the differential equation

$$dN/dt=\tilde{I}(t)-\beta N^2. \tag{7}$$

The inherent difference between the two cases is reflected in the different definitions of the probability factors α and β. The former has dimensions of frequency, but the latter those of volume times frequency.

It is well known that Eq. (7) is soluble for a stepped excitation function and leads to a hyperbolic decay characteristic. For sinusoidal modulation a useful approximate solution can be obtained for small depths of modulation. The experimental condition, $a\leqslant 0.1$, is already sufficient. The solution is given in Appendix A. It is shown that under this condition the emission modulation may be considered as closely sinusoidal especially since even harmonics are rejected by the homodyne measuring technique, and the third harmonic contribution is never bigger than the noise level. From the Appendix (A11) the in-phase attenuation factor is found to be

$$\chi=4\tilde{A}\beta/(4\tilde{A}\beta+\omega^2). \tag{8}$$

This will be recognized as having identical form to the monomolecular case (6), and when represented as in Fig. 1 the phosphorogram has a center of symmetry at the point $\{\frac{1}{2}, \log[2(\tilde{A}\beta)^{\frac{1}{2}}]\}$.

Four conclusions may be drawn thus far:

1. The simplest, i.e., one-process, mechanisms having either monomolecular or bimolecular kinetics should give the same elementary phosphorogram, Fig. 1, for small depth of modulation.

2. The accuracy of measurement should be sufficient to verify whether these simple mechanisms are a proper description of actual phosphors.

3. Measurement of phosphorograms with different average excitation intensities should distinguish unequivocally between a monomolecular and a bimolecular

process. The phosphorogram of the monomolecular process should be invariant, whereas that of the bimolecular process should move in the direction of higher frequencies with higher average intensities. The shift between two values of $\tilde{A}$, $\tilde{A}_1$ and $\tilde{A}_2$, should be

$$\tfrac{1}{2}\log(\tilde{A}_2/\tilde{A}_1).$$

4. Because $\tilde{A}$ is not an observable, the ratio $\tilde{A}_2/\tilde{A}_1$ may differ from A_2/A_1, and so the shift may not be exactly $\frac{1}{2}\log(A_2/A_1)$. Also the bimolecular probability β cannot be revealed by the phosphorogram alone since it is directly related to $\tilde{A}$ and not to A.

MORE COMPLEX SYSTEMS

Because of the considerable accuracy that is available in this kind of measurement, it may be expected that there will be an improved chance of disclosing more complex mechanisms in phosphorescence. Before considering actual phosphorescence mechanisms in the accepted terms of solid state physics, it is as well to treat from a mathematical point of view simple combinations of processes of the elementary type already discussed. This will serve to establish the qualitative features of their phosphorograms, for unless an intelligent operator can recognize such features in the phosphorograms of actual phosphors, there is little chance that a computing machine will economically reach a quantitative analysis by a method of systematic but unintelligent trials.

Cascaded Processes

Any attempt to describe the details of energy transfer through a phosphor from irradiation to emission will involve several processes in cascade. Many of these processes will be effectively instantaneous, and so will inevitably be undetectable by this method since no intermediate states are observable.

Now that the elementary equations (1) and (7) are solved, the analytical form of the phosphorogram of two processes in cascade may be deduced without recourse to the differential equation. If subscripts are used to distinguish the parameters of the component processes from those of the whole system, we have

$$\lambda=\lambda_1\lambda_2,$$

and

$$\phi=\phi_1+\phi_2,$$

whence

$$\begin{aligned}\chi&=\lambda_1\lambda_2\cos(\phi_1+\phi_2)\\&=(\alpha_1^2\alpha_2^2-\omega^2\alpha_1\alpha_2)/\{(\alpha_1^2+\omega^2)(\alpha_2^2+\omega^2)\}.\end{aligned}\tag{9}$$

The order of the components cannot be distinguished, so α_2 may be supposed larger than α_1 without loss of generality. Relation (9) may be simplified by the substitutions

$$\theta=\omega/\alpha_1$$

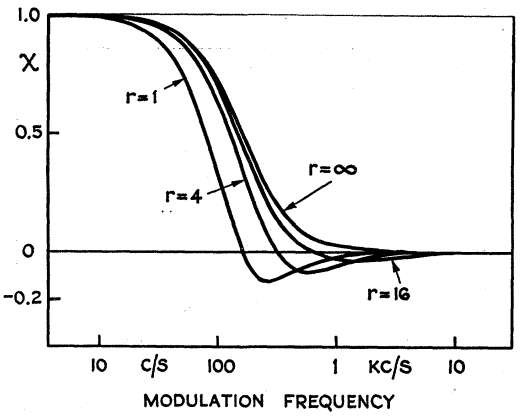

FIG. 2. Examples of phosphorograms of two simple processes in cascade for different ratios of their rate constants, 1000 and $1000r$ sec^{-1}.

and

$$r=\alpha_2/\alpha_1\gtrless 1,$$

to give

$$\chi=(1-\theta^2/r)/\{(1+\theta^2)(1+\theta^2/r^2)\}.\tag{10}$$

The phosphorogram of two cascaded processes is sketched in Fig. 2 with r as parameter. Unless r is large the appearance of a minimum makes the phosphorogram qualitatively distinct from that of the elementary process. In the limit $r\rightarrow\infty$, relation (10) reduces to (6), confirming the intuitive supposition that large separations between rate constants would make the faster process undetectable.

Concurrent Processes

Systems of concurrent processes are more complicated even when only a single pair is involved because there is a third parameter which measures the partition of incoming energy between the two components in addition to their two rate constants. It is convenient to introduce this ratio as the weight (p) of each component which is then fully defined by a number pair (p,α) giving its weight and rate constant. The weights can be presumed normalized.

The in-phase attenuation factors of each of a group of concurrent components may be added scalarly. With an obvious extension of the notation of the previous section we have the generalized relation

$$\chi=\textstyle\sum_i p_i\chi_i,\tag{11}$$

where

$$\chi_i=\alpha_i^2/(\alpha_i^2+\omega^2).$$

The advantage of using the parameter χ instead of either λ or ϕ will be clear if the expression for either is deduced even for a system of just two components.

The phosphorogram associated with relation (11) may be regarded as the convolution of the elementary phosphorogram (6) with a set of delta functions arranged along the axis of $\log\omega$ each with weight p_i at the position $\omega=\alpha_i$. By analogy with line emission spectra this set of

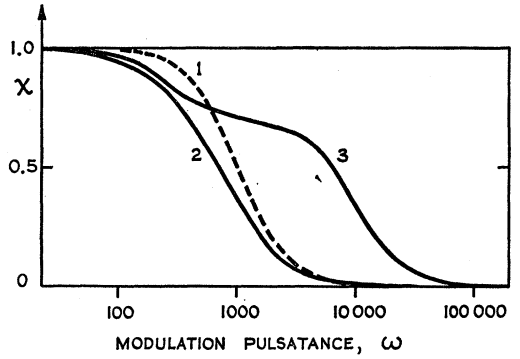

FIG. 3. Examples of phosphorograms of two concurrent simple processes compared with that of a single process (Fig. 1). Curve 1: $\alpha=1000$. Curve 2: $p_1=0.3$, $\alpha_1=250$; $p_2=0.7$, $\alpha_2=1000$. Curve 3: $p_1=0.3$, $\alpha_1=250$; $p_2=0.7$, $\alpha_2=10\,000$. The units of both α and ω are seconds^{-1}.

delta functions is called the *decay rate spectrum* of the phosphorogram, and is the more fundamental property of the phosphor. Analysis of such a phosphorogram into its decay rate spectrum is the familiar problem of deconvolution. The possibility of a successful solution is closely related to the accuracy and range of the experimental observations.

As in the case of cascaded processes, there are qualitative features of the phosphorogram which permit a group of concurrent processes to be recognized. At every value of the parameter χ the slope is *less* that that of the elementary phosphorogram (Fig. 1). Two examples are sketched in Fig. 3. In Fig. 4 one of these phosphorograms is shown in conjunction with its decay rate spectrum. The alternative horizontal scales show how the decay rate spectrum may be represented equally well on a frequency or time scale, but that there is a displacement of $\log 2\pi$ between it and the phosphorogram. The vertical boundaries mark the limits of the range accessible with the present instrumentation. Although the decay rates of components lying outside these limits are not observable, their combined weights can generally be determined.

Almost every phosphorogram so far recorded appears to be of this type, and may be analyzed as a discrete decay rate spectrum. It is surprising that there should be no clear evidence of cascaded processes, and also that discrete components should be found rather than a statistical distribution which might well have been expected.

A Hypothetical Example

In conclusion a hypothetical example will be given to illustrate the potentialities of the method. Let us suppose that excitation consists of raising electrons to a high excited state from which a proportion p_1 quickly reach a particular metastable state. The lifetime of this state (α_1^{-1}) is of the order of a millisecond (mid-range for the phosphorometer), and the transition to the ground state gives rise to observable emission. Suppose also that there is an associated trapping state which receives a proportion p_2 of the excited electrons, and releases them to the metastable state with probability α_2 per second. It is not necessary to normalize these weights since there may be other concurrent radiative components which cannot readily be distinguished by optical filtering. The α_1-process could be either entirely localized at the luminescence center (monomolecular), or involve a conduction band (bimolecular), but in either case it is likely to be only slightly temperature dependent. The trapping process could also be bimolecular, but in any case it should be strongly dependent upon temperature. Three main cases are qualitatively distinct:

Case I. $\alpha_1 \ll \alpha_2$.

The trapping process is not observable and the decay rate spectrum has a component at α_1 with weight (p_1+p_2).

Case II. $\alpha_2 \ll \alpha_1$.

The decay rate spectrum has two components (p_1,α_1) and (p_2,α_2).

Case III. $\alpha_1 \sim \alpha_2$.

If $p_1 \ll p_2$, then the phosphorogram has the features of a simple cascaded pair. If $p_2 \ll p_1$, the case reduces to Case I. Between these two limits the form of the phosphorogram may be seen from Fig. 2 by combining the curves "$r=\infty$" and "$r=4$" (for example) in proportions $p_1:p_2$. Although the characteristic minimum may disappear, the slope in the region $\omega \sim \alpha_1$ will always be too large for successful analysis as a simple decay rate spectrum.

The nature of both processes can be ascertained by varying the average exciting intensity. If α_2 is indeed a strong function of temperature it should be possible to cover at least two of the above cases by recording phosphorograms over a range of temperatures. It is however not obvious what temperature variations in p_1 and p_2

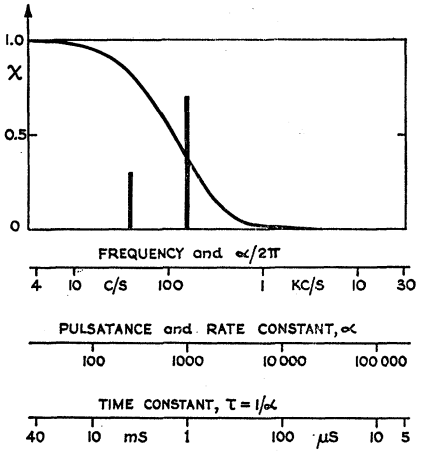

FIG. 4. The phosphorogram example 2 of Fig. 3 shown in conjunction with its decay rate spectrum with alternative horizontal scales. The vertical extremes represent the experimental limits of modulation frequency.

can be expected: If they are large the issue will be obscured. Nevertheless, the method should allow considerable progress to be made in elucidating the mechanism of phosphorescence.

ACKNOWLEDGMENT

It is a pleasure to acknowledge the patience and advice of Dr. A. L. G. Rees and the encouragement of Dr. C. K. Coogan and many other members of this Division.

APPENDIX A

The physical conditions for which the equation

$$dN/dt=\tilde{A}(1+a\cos\omega t)-\beta N^2 \qquad \text{(A1)}$$

was set up require that N is at all times positive, and further that after a steady state has been reached N must be a periodic function with the fundamental pulsatance ω of the excitation function $I(t)$. Thus the solution may be written as a Fourier series,

$$N=D\{1+\textstyle\sum_r(a_r\cos r\omega t+b_r\sin r\omega t)\}. \qquad \text{(A2)}$$

Because of the additional condition of small depth of modulation, $a\leqslant 0.1$, the rate of convergence of the expansion (A2) will be assumed to follow the set of inequalities

$$(a_1^2+b_1^2)^{\frac{1}{2}}<\tfrac{1}{2}a, \qquad \text{(A3)}$$

and

$$|a_r|,\quad |b_r|<(\tfrac{1}{2}a)^r, \qquad \text{(A4)}$$

for $r=2, 3, 4, \cdots$. With these assumptions it is possible to deduce approximate expressions for a_r and b_r. These expressions are then shown to be consistent with assumptions (A3) and (A4).

The term N^2 may also be written as a Fourier series,

$$\beta N^2=B\{1+\textstyle\sum_r(c_r\cos r\omega t+d_r\sin r\omega t)\}. \qquad \text{(A5)}$$

By squaring (A2) and identifying it with (A5), a set of relations between the Fourier coefficients is obtained, of which the first few are

$$\begin{aligned}
B&=\beta D^2\{1+\tfrac{1}{2}(a_1^2+b_1^2)+\cdots\},\\
Bc_1&=\beta D^2\{2a_1+(a_1a_2+b_1b_2)+\cdots\},\\
Bd_1&=\beta D^2\{2b_1+(a_1b_2-a_2b_1)+\cdots\},\\
Bc_2&=\beta D^2\{2a_2+\tfrac{1}{2}a_1^2-\tfrac{1}{2}b_1^2+(a_1a_3+b_1b_3)+\cdots\},\\
Bd_2&=\beta D^2\{2b_2+a_1b_1+(a_1b_3-a_3b_1)+\cdots\},\\
Bc_3&=\beta D^2\{2a_3+a_1a_2-b_1b_2+(a_1a_4+b_1b_4)+\cdots\\
&\qquad +(a_2a_3+b_2b_3)+\cdots\},\\
Bd_3&=\beta D^2\{2b_3+a_1b_2+a_2b_1+(a_1b_4-a_4b_1)+\cdots\\
&\qquad +(a_2b_3-a_3b_2)+\cdots\}.
\end{aligned} \qquad \text{(A6)}$$

Using the assumptions (A3) and (A4) in each of these expansions (A6) the terms preceding the parenthesis are of order a^r, the terms in parenthesis are of order a^{r+2}, and the remaining terms are of order a^{r+4} or smaller. Consequently, the error in neglecting all but the terms of order a^r is just more than 0.1% in the first relation, and much less in the remainder.

With these approximations, therefore, the coefficients a_r and b_r may be obtained by substituting (A5) and the differential coefficient of (A2) in the original equation (A1). Using the appropriate relations (A6) and equating coefficients for $r=0$ and $r=1$, we have

$$D=(\tilde{A}/\beta)^{\frac{1}{2}},$$

$$-\omega a_1D=-2\tilde{A}b_1,$$

and

$$\omega b_1D=\tilde{A}(a-2a_1).$$

The solution is

$$a_1=\tfrac{1}{2}a/(1+\xi^2), \qquad \text{(A7)}$$

and

$$b_1=\tfrac{1}{2}a\xi/(1+\xi^2), \qquad \text{(A8)}$$

where

$$\xi=\omega D/2\tilde{A}=\omega/2(\tilde{A}\beta)^{\frac{1}{2}}.$$

The expressions (A7) and (A8) are readily shown to be compatible with the assumption (A3). Combining (A7) and (A6) gives

$$c_1=a/(1+\xi^2). \qquad \text{(A9)}$$

Equating coefficients for $r=2$ gives

$$-2\omega a_2D=-\tilde{A}(2b_2+a_1b_1)$$

and

$$2\omega b_2D=-\tilde{A}(2a_2+\tfrac{1}{2}a_1^2-\tfrac{1}{2}b_1^2),$$

whence

$$a_2=(5\xi^2-1)a^2/16(1+4\xi^2)(1+\xi^2)^2,$$

and

$$b_2=\xi(\xi^2-2)a^2/8(1+4\xi^2)(1+\xi^2)^2.$$

These expressions can be shown to be compatible with assumption (A4) for $r=2$. Equating coefficients for $r=3$ in the same way shows again values compatible with (A4) for $r=3$, and further that

$$|\tfrac{1}{3}c_3|<0.1\%\text{ of }c_1 \qquad \text{(A10)}$$

for all values of ξ.

The homodyne detector (Part II) passes a signal proportional to

$$c_1+\tfrac{1}{3}c_3+\tfrac{1}{5}c_5+\cdots.$$

But on account of (A10) only the first term need be considered, so that the measured in-phase attenuation factor will be (from A9)

$$\chi=1/(1+\xi^2), \qquad \text{(A11)}$$

with a maximum error of order 0.1% which is the same as the error of measurement.